Pure and Applied Geophysics

CrossMark

Depth Estimation Method Based on the Ratio of Gravity and Full Tensor Gradient Invariant

Wenna Zhou[1,2]

Abstract—In this paper, I present a new depth estimation method based on the ratio of gravity and full tensor gradient invariant. The new approach is designed to be stably and quickly interpret the gravity data and full tensor gravity data. First, we deduce two simple calculation equations using the particular models (sphere and horizontal cylinder model). The depths of the particular sources can be directly calculated using the simple equations. However, a shape factor similar to the structural index of Euler deconvolution is contained in the simple calculation equations. It directly relates to the accuracy of calculation depth. To calculate the depth of source accurately, the shape factor must be determined first. Thus, the application of the simple equations is very circumscribed. To overcome the limitation, I calculate the ratio of the simple equations of different altitudes to improve the original algorithm. It effectively eliminates the influence of the shape factor. I use different model to test the method and apply the method on real gravity data. It demonstrates that the new approach is stable, simple and effective depth estimation method. The new improved approach not only can be used to calculate the sphere and cylinder model depth, but also can be used to calculate other general models. It is a very useful tool to calculate the depth of gravity bodies.

Key words: Gravity anomaly, full tensor gradient invariant, depth estimation.

1. Introduction

Gravity data capture the lateral density variations in the Earth. The advantage of the gravity data is its lateral resolution. However, a complete quantitative interpretation of gravity data usually needs three information: the depth, the dimension (the horizontal position) and the physical property. In many researches and applications, the depth is often a more important parameter needed to be estimated. Therefore, many depth estimation methods have been introduced, such as Euler deconvolution (Thompson 1982; Stavrev and Reid 2007, 2010), Naudy method (Naudy 1971), Werner deconvolution (Hartman et al. 1971; Hansen 2005), analytic signal-based methods (Nabighian 1972; Roest et al. 1992; Bastani and Pedersen 2001), local wave-number methods (Thurston and Smith 1997; Keating 2009), and wavelets methods (Cooper 2006). These methods have been proved very useful and effective in gravity data depth interpretation.

In the ongoing development of full tensor gravity gradiometry (FTG) technique, more and more FTG data are routinely used in exploration programs to evaluate and explore geological structures. The FTG data have many advantages so that more and more researchers began to propose new interpretation method for FTG data (Hayes et al. 2008; Cevallos et al. 2013; Oliveira and Barbosa 2013). Many methods for FTG data are evolved from the methods for gravity data. Simultaneously, the gradient components are widely used in interpretation of gravity data. For example, the popular approach of Euler deconvolution method was originally implemented using the three gradient components of vertical direction. Then, it was developed into the gradient tensor form to interpret gravity and FTG data by (Zhang et al. 2000). The same as Euler deconvolution method, Tilt-depth method also was modified to interpret FTG data (Salem et al. 2013). Analytic signal method for FTG data was established (Beiki 2010). Meanwhile, these new proposed methods displayed the advantages of using multi-components of FTG (measured or calculated) to interpret gravity data and not FTG data.

[1] *Present Address*: Key Laboratory of Mineral Resources in Western China (Gansu Province), School of Earth Sciences, Lanzhou University, Lanzhou 730000, Gansu, China. E-mail: wennazhou@163.com
[2] College of Geo-exploration Science and Technology, Jilin University, Changchun 130026, Jilin, China.

The full tensor gradient invariants are important tool to interpret FTG data. PEDERSEN and RASMUSSEN (1990) proposed three invariants I_0, I_1 and I_2, and discussed the advantages of the invariants in gravity and FTG data interpretation. MATARAGIO and KIELEY (2009) used various invariants to interpret the FTG data. ORUÇ (2010) has established a depth estimation method from FTG invariants and vertical component. BEIKI and PEDERSEN (2010) used eigenvector of gradient tensor to locate geologic bodies. All of these methods can display the advantages of the invariants in gravity and FTG data interpretation.

In this paper, I propose a new depth estimation method based on the ratio of gravity and FTG invariant. The method is first established based on the simple sphere and cylinder model, and then it is improved using different altitudes data. Thus, the influence of shape factor that is related to the model shape is discarded. The new method is tested using various model data and real measured gravity data.

2. Theory

2.1. Mathematical Background of FTG and the Invariants

The gravity gradient tensor Γ can be defined as:

$$\Gamma = \begin{bmatrix} \frac{\partial^2 U}{\partial x^2} & \frac{\partial^2 U}{\partial x \partial y} & \frac{\partial^2 U}{\partial x \partial z} \\ \frac{\partial^2 U}{\partial y \partial x} & \frac{\partial^2 U}{\partial y^2} & \frac{\partial^2 U}{\partial y \partial z} \\ \frac{\partial^2 U}{\partial z \partial x} & \frac{\partial^2 U}{\partial z \partial y} & \frac{\partial^2 U}{\partial z^2} \end{bmatrix} = \begin{bmatrix} g_{xx} & g_{xy} & g_{xz} \\ g_{yx} & g_{yy} & g_{yz} \\ g_{zx} & g_{zy} & g_{zz} \end{bmatrix} \quad (1)$$

U is the gravitational potential, and it satisfies Laplace's equation outside of source. $\nabla^2 U(r) = 0$, where g is the gravity vector.

PEDERSEN and RASMUSSEN (1990) have introduced the tree invariants for the potential field gradient tensors, which can be defined as follows:

$$I_0 = \text{trace}(\Gamma) = g_{xx} + g_{yy} + g_{zz} = 0 \quad (2)$$

$$I_1 = g_{xx}g_{yy} + g_{yy}g_{zz} + g_{xx}g_{zz} - g_{xy}^2 - g_{yz}^2 - g_{xz}^2 \quad (3)$$

and

$$\begin{aligned} I_2 &= \det(\Gamma) \\ &= g_{xx}(g_{yy}g_{zz} - g_{yz}^2) + g_{xy}(g_{yz}g_{xz} - g_{xy} - g_{zz}) \\ &\quad + g_{xz}(g_{xy}g_{yz} - g_{xz}g_{yy}) \end{aligned} \quad (4)$$

The invariants can be used to enhance and detect the edges and structures of geologic sources. They were widely used in potential field data interpretation.

2.2. Depth Estimation of Simple Models

2.2.1 The Point Source Model (Sphere Model)

PEDERSEN and RASMUSSEN (1990) have introduced the gravity tensor equation of point source as follows:

$$\Gamma = -\frac{GM}{R^3} \begin{bmatrix} -1 + 3\xi^2 & 3\xi\eta & 3\xi\zeta \\ 3\xi\eta & -1 + 3\eta^2 & 3\eta\zeta \\ 3\xi\zeta & 3\eta\zeta & -1 + 3\zeta^2 \end{bmatrix} \quad (5)$$

where $(\xi, \eta, \zeta) = (x, y, z)/R$, then the invariants can be denoted as:

$$I_1 = -3\left(\frac{GM}{R^3}\right)^2 \quad (6)$$

$$I_2 = \text{Det}(\Gamma) = -2\left(\frac{GM}{R^3}\right)^3 \quad (7)$$

The gravity anomaly of sphere model can be calculated by:

$$g_z = GM\frac{h}{R^3} \quad (8)$$

where G is the gravitational constant, M is the mass, R is the radius and h is the depth. Then, we can obtain the depth calculation equation using Eqs. (6) and (8).

$$h = \left|\frac{\sqrt{3}g_z}{\sqrt{-I_1}}\right| \quad (9)$$

2.2.2 Line of Monopoles (Horizontal Cylinder Model)

As above, the gradient tensor components of horizontal cylinder can be obtained:

$$\Gamma = -\frac{GM}{R^2} \begin{bmatrix} 1 - 2\xi^2 & -2\xi\zeta \\ -2\xi\zeta & 1 - 2\zeta^2 \end{bmatrix} \quad (10)$$

where $(\eta, \zeta) = (y, z)/R$, and the invariant can be denoted as:

$$I_1 = -\left(\frac{2GM}{R^2}\right)^2 \quad (11)$$

As we all know, the gravity anomaly of horizontal cylinder can be denoted as:

$$g_z = 2GM\frac{h}{R^2} \qquad (12)$$

As mentioned above, where G, M, h, and R denote the gravitational constant, mass, radius and depth, in turn. Therefore, we can get the depth calculation equation as follows:

$$h = \left|\frac{g_z}{\sqrt{-I_1}}\right| \qquad (13)$$

Equations (9) and (13) have the similar form, and we rewrite them as a uniform form as follows:

$$h = \left|\frac{\sqrt{N}g_z}{\sqrt{-I_1}}\right| \qquad (14)$$

where N is the shape factor, it is a parameter related to the shape of model. For the simple model or geologic bodies, the depth can be directly calculated using Eqs. (9) and (13).

2.3. Improved Theory and the Workflow

2.3.1 Eliminating the Shape Factor and Automatically Obtaining the Depth

If a priori information concerning the source geometry has been known, as discussed in the preceding section, it is easy to calculate depth of geologic source. Equation (14) contains a shape factor. It means that the depth calculation result would be influenced by the shape factor. Different models need different shape factor that can result in different depth result. However, in the practical applied, the shape factor needs to be determined before depth calculation. It is difficult to determine the shape factor. Therefore, to discard the influence of shape factor is a preferable way. Given this, I deduce a new automatic calculation method without the shape factor.

In Eq. (14), g_z and I_1 are the gravity anomaly and the full tensor invariant, respectively. They are measured on ground (or on an original surface). The buried depth of geologic body is h. If the measured surface at another height is t, i.e., the distance between geologic body and the measured surface is $h + t$. We can get the gravity anomaly g'_z

and the invariant I'_1 of the measured surface t. The values can be obtained by upward continuation or can be directly obtained by airborne measure. Therefore, the distance from the source to the measure surface can be denoted as:

$$h + t = \left|\frac{\sqrt{N}g'_z}{\sqrt{-I'_1}}\right| \qquad (15)$$

Combining Eqs. (14) and (15), we can get:

$$\frac{h}{h+t} = \frac{\left|\frac{\sqrt{N}g_z}{\sqrt{-I_1}}\right|}{\left|\frac{\sqrt{N}g'_z}{\sqrt{-I'_1}}\right|} = \frac{\left|g_z/\sqrt{-I_1}\right|}{\left|g'_z/\sqrt{-I'_1}\right|} \qquad (16)$$

Assuming $GI = \frac{\left|g_z/\sqrt{-I_1}\right|}{\left|g'_z/\sqrt{-I'_1}\right|}$, we can eliminate the influence of N, and get the depth of geologic body:

$$h = \frac{|GI \times t|}{|1 - GI|} \qquad (17)$$

It is important to note, when the denominator equals zero, the singular point needs to be eliminated in calculation process. In addition, during the calculation, the altitude of upward continuation needs to be limited in a certain range. If the altitude is too small, the difference of the data of two altitudes cannot be displayed. However, if the altitude is too big, some of the detailed information of original data would be eliminated and the background effect would be increased. Therefore, the altitude of upward continuation is generally given as 1–3 sampling interval.

2.3.2 The Procedure of the New Method

In this method, the total horizontal derivative (THD) is adopted to outline the edge and confirm the location of geologic source. The maximum points are extracted using the algorithm introduced by BLAKELY and SIMPSON (1986). Therefore, the procedure of this new approach is shown in Fig. 1

At first, the gravity data or FTG data of ground need to be obtained. It is well known that gravity data can be transformed into FTG data and vice versa (LI 2001; SANCHEZ et al. 2005; DRANSFIELD 2010). Then, we need to calculate the invariant I_1 and determine the center position of geologic source. Furthermore, the gravity and FTG data of another altitude t can be calculated by the upward

continuation. Because the upward continuation is similar to the low-pass filter, the upward continuation of FTG data can be implemented using the noise reduction procedures (PILKINGTON and SHAMSIPOUR 2014). The authors pointed out the least-squares estimation of common gravity potential from which each component can be subsequently recalculated (LI 2001; SANCHEZ et al. 2005; DRANSFIELD 2010). Any residual noise effects in the data that are not Laplacian will be removed with this procedure. Conversely, any noise components that do satisfy Laplace's equation will remain unaffected. Alternatively, there are the corresponding airborne data, and the different altitudes data need to be interpolated to a uniform grid. Then, we only need to extract the gravity and I_1 value of different height, and use Eq. (17) to calculate the depth.

Meanwhile, from the workflow, one can see that the depth of geologic bodies can be obtained using different altitudes data. FLORIO et al. (2014) have proved that upward continuation is an effect tool to improve the accuracy of depth estimation. Therefore, if the original data are seriously interfered by noise, we can eliminate the noise by upward continuation, and then calculate the depth using the workflow. The depth of source equal to the calculated result subtracts the altitude of upward continuation.

3. Synthetic Model Tests

3.1. Simple Model Without Random Noise

To test the reliability and accuracy of the new method, I first present sphere and horizontal cylinder models to calculate depth, respectively. The forward calculated formulation was given by BLAKELY (1995).

Model 1 contains two different spheres. The parameters of the sphere model are: the radius $R1 = 20$ m, $R2 = 50$ m, the depths $h1 = 50$ m, $h2 = 150$ m, all of the density contrasts are 1 g/cm^3. The sampling interval is 10 m. Figure 2a shows the gravity anomaly of the model, and Fig. 2b shows the I_1 of the gravity data. Meanwhile, the total horizontal derivative is calculated to locate the positions of the spheres (Fig. 2c, d).

I first calculate the sphere depth using Eq. (9) with the shape factor 3, and the depth result is shown in Fig. 2c. It can be seen that the result corresponds with the real depth of sphere. This demonstrates that if the shape factor can be obtained as a prior parameter, the depth can be calculated accurately. Figure 2d shows the depth result calculated using Eq. (17). The upward continuation height is 10 m. From the result, we can see that the depths
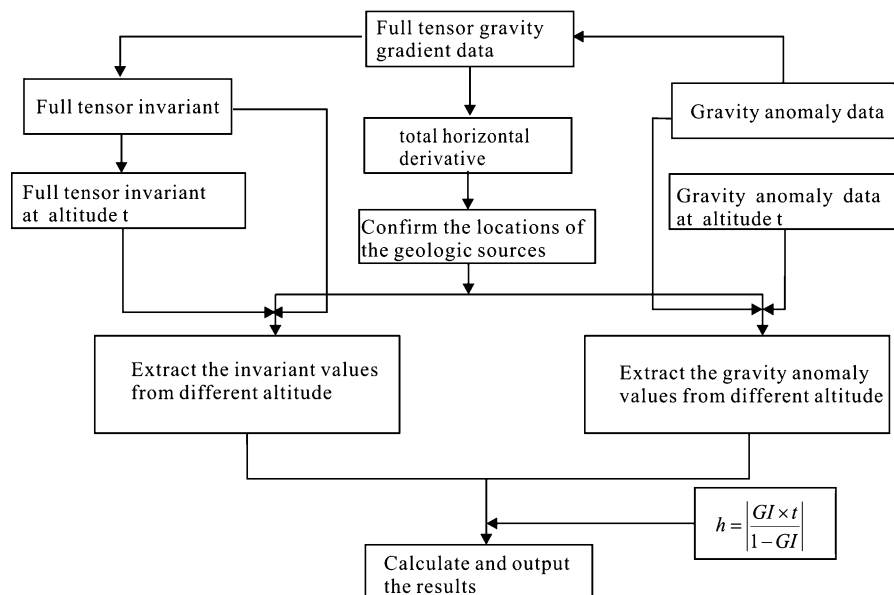

Figure 1
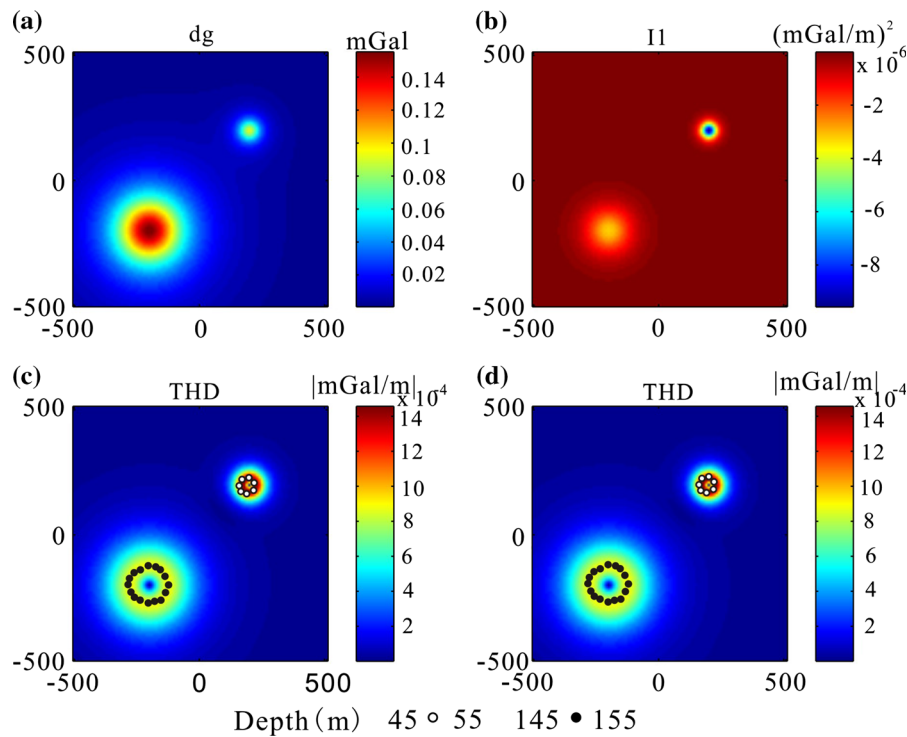The calculation workflow of the depth estimation method

Figure 2
a Gravity anomaly of model 1. **b** The full tensor invariant I_1. **c** The total horizontal derivative and depth calculated using Eq. (9) with the shape factor equal to 3, where the *white* and *black dots* denote depth. **d** The total horizontal derivative and depth calculated using Eq. (17) without the shape factor, where the *white* and *black dots* denote depth

correspond with Fig. 2c and they agree well with the real depth of spheres. It is thus clear that the improved approach is effective in depth calculation.

For the 2-D situation, I establish horizontal cylinder model to test the approach. The parameters of the model are: the radius $R1 = 10$ m, $R2 = 20$ m, the depths $h1 = 100$ m, $h2 = 200$ m, and the density contrast is 1 g/cm^3. The sampling interval is 10 m. The same as above, I use the two methods to calculate depths of the cylinders. The results are shown in Fig. 3. Figure 3a is the gravity anomaly of the two cylinders. I_1 is calculated and shown in Fig. 3b. The positions of the cylinders can be produced by the maximum of the THD. Then, I calculate the depth by Eq. (14) with the shape factor 1, and the result is shown in Fig. 3c. Finally, I calculate the depth using Eq. (17) with the upward continuation altitudes 10 m. The result is shown in Fig. 3d. It is corresponding with the Fig. 3c. Both of the results correspond well with the real depths.

It demonstrates that both of the method can obtain the depth result of geologic source.

3.2. Complex Model with Random Noise

To further study the practicability of the new approach, I use a complex model composed of sphere (body 1), vertical prism (body 2) and vertical cylinder (body 3), and their horizontal edge positions are shown by dashed lines. The buried depth of vertical prism is 200–800 m, and the vertical cylinder is 400–800 m. The center depth of sphere is 400 m. All of the density contrasts are 1 g/cm^3. I add the 0.5 % of the maximum amplitude Gaussian noise, and the anomaly is shown in Fig. 4a. The invariant I_1 is shown in Fig. 4b. For the noise data, it is difficult to accurately calculate the depth of geologic source (FLORIO *et al.* 2014). Meanwhile, it is inaccurate to obtain the positions of models using the THD with noise (Fig. 4c). To obtain the depth
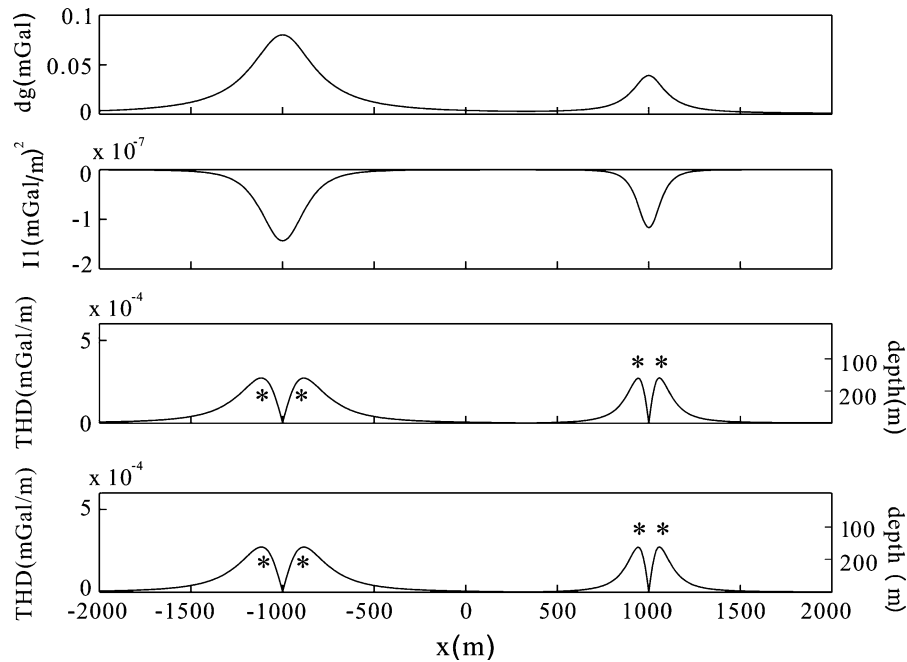
Figure 3
a Gravity anomaly of model 2. **b** The full tensor invariant I_1. **c** The depth calculated using Eq. (14) with the shape factor equal to 1, where the *asterisks* denote the depth. **d** The depth calculated using Eq. (17) without the shape factor, where the *asterisks* denote the depth

accurately, the upward continuation is calculated first (the altitude of upward continuation is 30 m). Then, the positions of the model can be obtained using the maximum values of THD (Fig. 4d). The depth is calculated using the workflow, and the result is shown in Fig. 4d. From the result, it can be seen that the calculated depth mainly displays the center depth of geologic sources. All of the models' depths agree with the real buried depths. It demonstrates that the new approach is utility for depth estimation. The upward continuation can be used to denoise and improve the accurate of this approach.

3.3. Test the Noise Influence

To further capture the noise influence of the new approach, I use a 2D model that consists of two dikes, and Gaussian random noise with different amplitude is added. The top depths of two dikes are 15 and 20 m, respectively. The density contrast of both is 1 g/cm³. The sample interval is 2 m. First, I directly calculate the depth of the model without noise using the workflow, and the result is shown in Fig. 5c. The calculated depth agrees with the real depth. Then,

Gaussian random noises with 0 mean and standard deviation of 1, which are equal to 2 % of the maximum data amplitude, have been added in the gravity data (Fig. 6a). To obtain the maximum value of THD conveniently, upward continuation data at 3 sampling intervals (i.e., 6 m) have been obtained first, and then the depth can be calculated using the workflow. The result is shown in Fig. 6c. A more serious Gaussian random noise is added in the data (the amplitude is 5 % of the maximum data amplitude) (Fig. 7a), and to filter the noise, higher altitude (5 sampling intervals) is used in this test. The depth result is shown in Fig. 7c. It can be seen that with the increase of noise amplitude, the error of depth result is increased as well. However, the results still can be used to denote the depth range of geologic source. It demonstrates that the upward continuation is a useful way to reduce the noise influence in this method.

4. Real Data Examples

To demonstrate the application effect, the new method is applied to gravity data from Texas, which
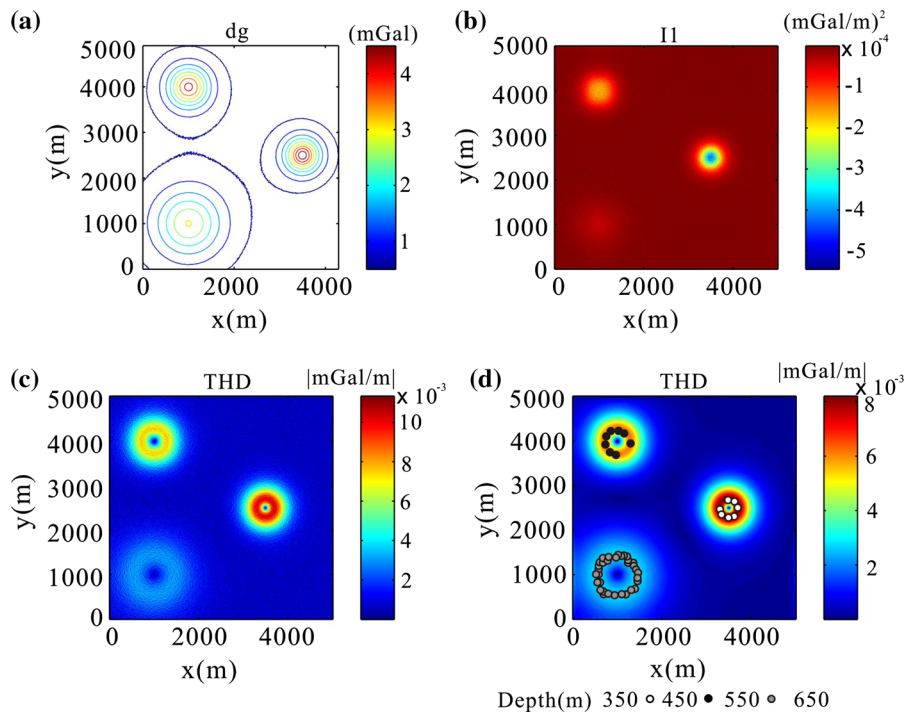
Figure 4
a Gravity anomaly of model 3, the amplitude of Gaussian noise equal to 0.5 % of the maximum amplitude of the data. **b** The full tensor invariant I_1 of the noised data. **c** The THD of the noised data without upward continuation. **d** The THD of the noised data with 30 m upward continuation and the depth calculated using Eq. (17)
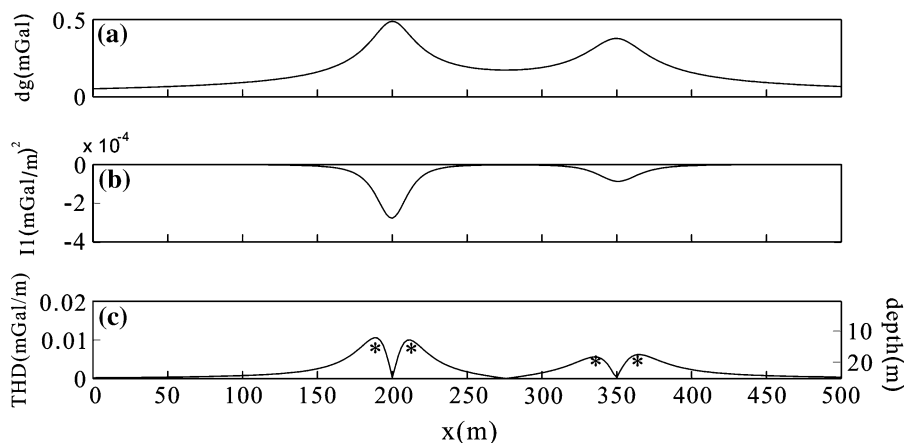

Figure 5
a Gravity anomaly of the dyke model. **b** The full tensor invariant I_1. **c** The depth calculated using Eq. (17) without the shape factor, where the *asterisks* denote the depth
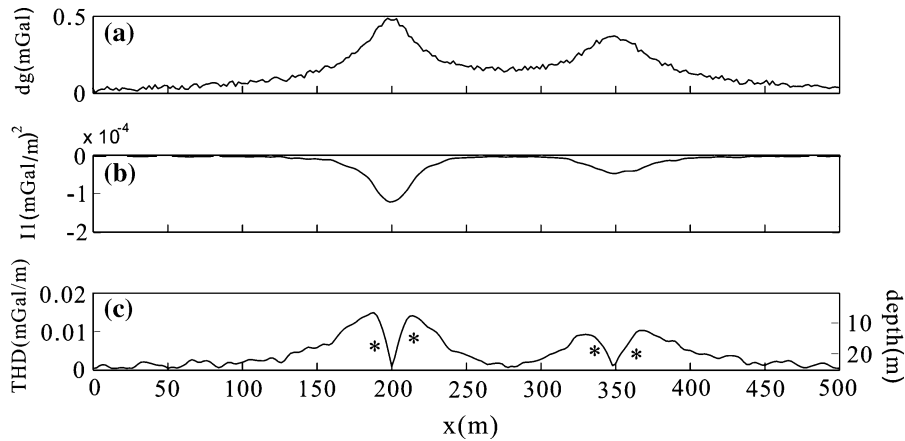
Figure 6
a Gravity anomaly of the dyke model with the amplitude is 2 % of the maximum data amplitude. **b** The full tensor invariant I_1 of the noised data. **c** The depth calculated using Eq. (17) without the shape factor, where the *asterisks* denote the depth
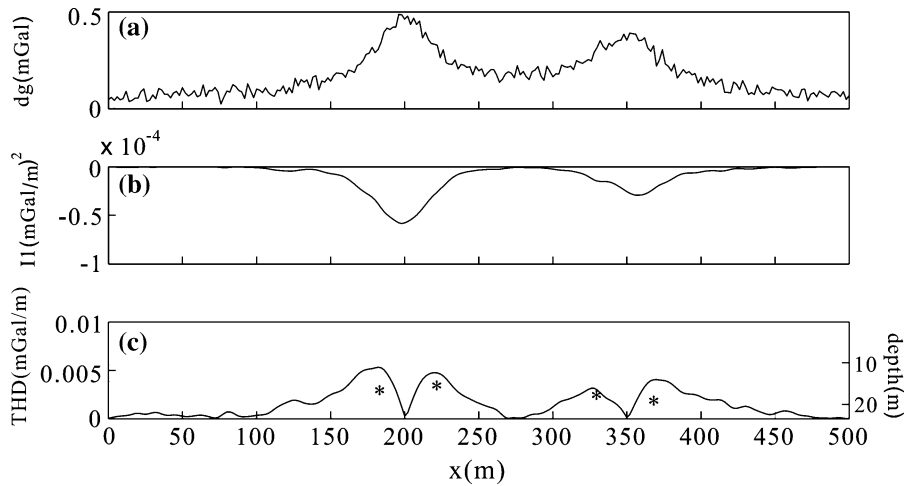

Figure 7
a Gravity anomaly of the dyke model with the amplitude is 5 % of the maximum data amplitude. **b** The full tensor invariant I_1 of the noised data. **c** The depth calculated using Eq. (17) without the shape factor, where the *asterisks* denote the depth
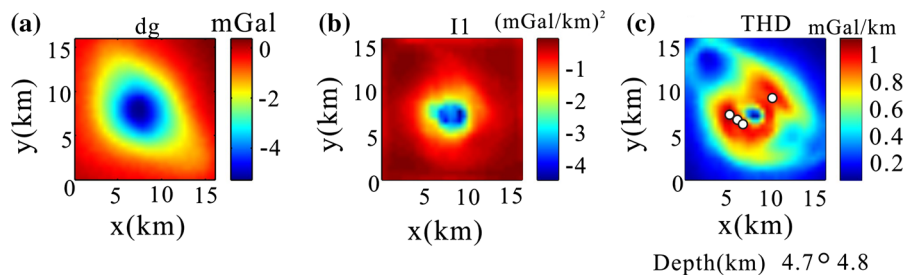

Figure 8
a The residual gravity anomaly of research area. **b** The full tensor invariant I_1. **c** The THD of the data and the depth calculated using Eq. (17)

Table 1

The depth results of the gravity data from different studies

Method from different researches	Depth/km
(Nettleton 1976)	4.97
(Mohan *et al.* 1986)	4.63
(Abdelrahman *et al.* 1991)	4.65
(Shaw and Agarwal 1997a)	4.13
(Salem *et al.* 2004)	5.12
(Essa 2007)	4.18
(Oruç 2010)	4.12

was digitized from a residual Bouguer anomaly map (Shaw and Agarwal 1997b, c). The interval of the grid data is 500 m, and the Bouguer anomaly map is shown in Fig. 8a. Several authors used different methods to interpret this Bouguer anomaly. Moreover, there was an array of seismic and drilling information to verify our conclusion.

Figure 8b shows the invariant I_1, and I calculated the THD to use its maximum to confirm the positions of geologic bodies. Then, I calculate the depth of geologic sources using the above workflow. The result is shown in Fig. 8c. The depth is about 4.7–4.8 km. I compare the result with other author's research (Table 1), it displays that the new calculated result is reasonable and accuracy. It demonstrates that the present approach is very useful to interpret the gravity data.

5. Conclusions

Full tensor invariants play an important role in gravity and FTG data interpretation. The invariants can be used to delineate the edges of geologic sources and to outline the feature of geological structures. More importantly, they have many advantages in data interpretation for the character that they are invariant with the axis rotation. In this paper, I proposed a new simple depth estimation method using the FTG invariant. The new method can calculate the depth of geologic source without any prior information. The depth of geologic source can be directly calculated using different altitudes data. Model test demonstrated that this new method is accurate in the sphere and horizontal cylinder depth estimation. In addition, for the other general model, the depth also can be

obtained by this method. It is worth mentioning that the new method can decrease the noise influence by the upward continuation. Finally, the method was applied to a real gravity data. The calculated result agreed well with the previous researches. All of the results demonstrated that the new method is accurate and effective in depth estimation. The proposed technique can be routinely applied to regional interpretation.

References

Abdelrahman, E., Bayoumi, A. and El-Araby, H. (1991), *A least-squares minimization approach to invert gravity data*, Geophysics, *56*, 115–118.

Bastani, M. and Pedersen, L. B. (2001), *Automatic interpretation of magnetic dike parameters using the analytical signal technique.*, Geophysics, *66*, 551–561.

Beiki, M. (2010), *Analytic signals of gravity gradient tensor and their application to estimate source location*, Geophysics, *75*, I59–I74.

Beiki, M. and Pedersen, L.B. (2010), *Eigenvector analysis of gravity gradient tensor to locate geologic bodies*, Geophysics, *75*, I37–I49.

Blakely, R. J. (1995), Potential theory gravity and magnetic applications, Cambridge: Cambridge University Press.

Blakely, R. J. and Simpson, R. W. (1986), *Approximating edges of source bodies from magnetic or gravity anomalies*, Geophysics, *51*, 1494–1498.

Cevallos, C., Kovac, P. and Lowe, S.J. (2013), *Application of curvatures to airborne gravity gradient data in oil exploration*, Geophysics, *78*, G81–G88.

Cooper, G.R.J. (2006), *Interpreting potential field data using continuous wavelet transforms of their horizontal derivatives.*, Computers&Geosciences, *32*, 984–992.

Dransfield, M. (2010), *Conforming Falcon gravity and the global gravity anomaly*, Geophysical prospecting, *58*, 469–483.

Essa, K.S. (2007), *Gravity data interpretation using the s-curves method*, Journal of Geophysics and Engineering, *4*, 204.

Florio, G., Fedi, M., Pasteka, R. (2014), *On the estimation of the structural index from low-pass filtered magnetic data*, Geophysics, *79*, 367–380.

HANSEN, R.O. (2005), *3D multiple-source Werner deconvolution for magnetic data*, Geophysics, *70*, L45–L51.

HARTMAN, R.R., TESKEY, D.J. and FRIEDHERG, J.L. (1971), *A system for rapid digital aeromagnetic interpretation*, Geophysics, *36*, 891–918.

HAYES, T.J., TIAMPO, K.F., FERNANDEZ, J. and RUNDLE, J.B. (2008), *A gravity gradient method for characterizing the post-seismic deformation field for a finite fault*, Geophysical Journal International, *173*, 802–805.

KEATING, P. (2009), *Improved use of local wavenumber in potential filed interpretation.*, Geophysics, *74*, 75–85.

LI, Y. (2001), Processing gravity gradiometer data using an equivalent source technique, Expanded Abstract, 71st Annual International Meeting, Soc. of Explor. Geophy.

MATARAGIO, J., KIELEY, J. (2009), *Application of full tensor gradient invariants in detection of intrusion-hosted sulphide mineralization: implications for deposition mechanisms.* First break, *27*, 95–98.

MOHAN, N., ANANDABABU, L. and RAO, S.S. (1986), *Gravity interpretation using the Mellin transform*, Geophysics, *51*, 114–122.

NABIGHIAN, M.N. (1972), *The analytic signal of two dimensional magnetic bodies with polygonal cross-section - Its properties and use of automated anomaly interpretation.*, Geophysics, *37*, 507–517.

NAUDY, H. (1971), *Automatic determination of depth on aeromagnetic profiles.*, Geophysics, *36*, 717–722.

NETTLETON, L.L. (1976), *Gravity and magnetics in oil prospecting,* edn, Vol. *464*, pp. Pages, McGraw-Hill New York.

OLIVEIRA, V.C., Jr. and BARBOSA, V.C.F. (2013), *3-D radial gravity gradient inversion*, Geophysical Journal International, *195*, 883–902.

ORUÇ, B. (2010), *Depth estimation of simple causative sources from gravity gradient tensor invariants and vertical component*, Pure and applied geophysics, *167*, 1259–1272.

PEDERSEN, L.B. and RASMUSSEN, T.M. (1990), *The gradient tensor of potential field anomalies: Some implications on data collection and data processing of maps*, Geophysics, *55*, 1558–1566.

PILKINGTON, M. and SHAMSIPOUR, P. (2014), *Noise reduction procedures for gravity-gradiometer data*, Geophysics, *79*, G69–G78.

ROEST, W.R., VERHOEF, J. and PIKINGTON, M. (1992), *Magnetic interpretation using the 3_D analytic signal.,* Geophysics, *57*, 116–125.

SALEM, A., RAVAT, D., MUSHAYANDEBVU, M.F. and USHIJIMA, K. (2004), *Linearized least-squares method for interpretation of potential-field data from sources of simple geometry*, Geophysics, *69*, 783–788.

SALEM, A., MASTERTON, S., CAMPBELL, S., FAIRHEAD, J.D., DICKINSON, J. and MURPHY, C. (2013), *Interpretation of tensor gravity data using an adaptive tilt angle method*. Geophysical Prospecting, *61*, 1065–1076.

SANCHEZ, V., SINEX, D. LI, Y., NABIGHIAN, M., WRIGHT, D., and SMITH, D. (2005), Processing and inversion of magnetic gradient tensor data for UXO applications: 18th EEGS Symposium on the Applications of Geophysics to Engineering and Environmental Problems, Extended Abstracts, 1193–1202.

SHAW, R. and AGARWAL, B. (1997a), *A generalized concept of resultant gradient to interpret potential field maps*, Geophysical prospecting, *45*, 1003–1011.

SHAW, R.K. and AGARWAL, B.N.P. (1997b), *A generalized concept of resultant gradient to interpret potential field maps*, Geophysics, *45*, 1003–1011.

SHAW, R.K. and AGARWAL, B.N.P. (1997c), *A generalized concept of resultant gradient to interpret potential field maps*, Geophysical Prospecting, *45*, 1003–1011.

STAVREV, P. and REID, A. (2007), *Degrees of homogeneity of potential fields and structural indices of Euler deconvolution*, Geophysics, *72*, L1–L12.

STAVREV, P. and REID, A. (2010), *Euler deconvolution of gravity anomalies from thick contact/fault structures with extended negative structural index*, Geophysics, *75*, I51–I58.

THOMPSON, D.T. (1982), *EULDPH: A new technique for making computer assisted depth estimates from magnetic data.*, Geophysics, *47*, 31–37.

THURSTON, J.B. and SMITH, R. S. (1997), *Automatic conversion of magnetic data to depth, dip, and susceptibility contrast using the SPI (TM) method.*, Geophysics, *62*, 807–813.

ZHANG, C.Y., MUSHAYANDEBVU, M.F., REID, A.B., FAIRHEAD, J.D. and ODEGARD, M.E. (2000), *Euler deconvolution of gravity tensor gradient data*, Geophysics, *65*, 512–520.